

New method for determining tie-lines in coexisting membrane phases using spin-label ESR

Yun-Wei Chiang^a, Jiang Zhao^b, Jing Wu^b, Yuhei Shimoyama^{a,1},
Jack H. Freed^a, Gerald W. Feigenson^{b,*}

^a*Baker Laboratory of Chemistry and Chemical Biology, and National Biomedical ACERT Center for Advanced ESR Technology, Cornell University, Ithaca, New York 14853-1301, USA*

^b*Department of Molecular Biology and Genetics, Cornell University, Ithaca, New York 14853, USA*

Received 30 August 2004; received in revised form 2 November 2004; accepted 16 November 2004

Available online 2 December 2004

Abstract

A full description of coexisting phases includes their respective compositions, which are provided by the thermodynamic tie-lines. Fluorescence microscopy enables visualization of coexisting lipid phases in giant unilamellar phases, but the composition information is missing. For cholesterol-containing lipid mixtures, knowledge of the compositions of the coexisting phases is important for understanding the nature of “membrane rafts”. We propose and demonstrate a new method, based on ESR spectroscopy, for determining tie-lines in regions of two-phase coexistence in a ternary lipid mixture. Over 100 different lipid compositions containing the spin-labeled phospholipid 16-PC in or near the two-phase coexistence region of the liquid-disordered and the gel phases of dipalmitoyl-PC/dilauroyl-PC/cholesterol (DPPC/DLPC/Chol) were studied to determine five tie-lines, spread over virtually the full range of this coexistence region. The method is based on the facts that (1) along a tie-line the ESR spectrum must be a superposition of the two ESR spectra from the respective single phases at the phase boundaries (connected by the tie-line) in a ratio given by the lever rule; (2) along a tie-line the partition coefficient, K_p , for the spin-label, which is also determined in our method, must be constant. We do find that K_p for 16-PC is close to unity, but its value depends on the particular tie-line. The coexisting phases in equilibrium are characterized by the K_p of the spin-label and its respective dynamic parameters obtained from fitting the ESR spectra to dynamical models.

© 2004 Elsevier B.V. All rights reserved.

Keywords: Tie-line; Partition coefficient; Membrane phase coexistence; ESR; Ternary lipid mixture

1. Introduction

Nonrandom mixing of lipid bilayer components is especially interesting when domains of different composition coexist. In particular, so-called lipid rafts seem to play important roles in functions of cell membranes such as signaling, protein transport, endocytosis and adhesion [1]. One aspect of raft formation in cell membranes is whether

there is actual lateral separation of lipids into coexisting liquid phases, i.e., liquid-ordered (L_o) and liquid-disordered (L_α) phases. Detection of coexisting lipid bilayer phases in vesicles has been accomplished by a variety of methods, such as fluorescence techniques [2–4] and ESR methods [5]. However, the compositions of the coexisting phases have been exceedingly difficult to determine [6]. The present study does not examine the region of coexistence of L_o+L_α phases, which might be a good model of lipid rafts, and instead focuses on method development in the most tractable region of the phase diagram.

Previous investigations by fluorescence and ESR techniques showed the coexistence of phases in model membrane vesicles, but did not quantitatively analyze the composition

* Corresponding author. Tel.: +1 607 255 4744; fax: +1 607 255 2428.

E-mail address: gwf3@cornell.edu (G.W. Feigenson).

¹ On leave from Department of Physics, Hokkaido University of Education, Hakodate 040-8567, Japan.

of each coexisting phase in order to determine tie-lines in phase coexistence regions. The goal of the present investigation was to develop a method for determining tie-lines in two-phase coexistence regions in a three-component lipid mixture. Methods for tie-line determination in ordinary three-component mixtures include the method of analysis and the method of titration. Such methods can be traced back to early work [7–10]. A series of investigations on the liquid–liquid equilibrium system that gives an excellent review of experimental analysis and prediction of phases in equilibrium can be found in the literature [11–13]. An important characteristic that all of these systems have in common is the relative ease of adding or removing the phases that are in equilibrium, making possible the determination of tie-lines in ternary equilibrium mixtures. However, for the lipid mixture of current interest, dipalmitoyl-PC/dilauroyl-PC/cholesterol (DPPC/DLPC/Chol), it is impossible to employ the above methods to separate the conjugate phases in equilibrium, precluding direct analysis of the respective coexisting phases. In earlier work, we reported the ternary phase diagram of DPPC/DLPC/Chol from measurements of FRET, confocal fluorescence microscopy, and dipyrène-PC excimer/monomer ratios [14]. We then mapped out the dynamic structure of the phase diagram using ESR spectral simulations [15]. In this report, we present a new method of tie-line determination using spin-labeling ESR, and we have determined the tie-lines in the liquid-disordered phase and gel phase coexistence region. This new method should be useful in finding tie-lines in other two-phase coexistence regions of lipid membrane systems. Potentially, characterization of “lipid raft mixtures” could be taken to a much higher level than has been previously achieved, such that the compositions of both coexisting phases are precisely established.

2. Materials and methods

2.1. Materials

Phospholipids (DPPC and DLPC), cholesterol and the spin label 1-palmitoyl-2-(16-doxyl stearoyl) phosphatidylcholine (16-PC) were purchased from Avanti Polar Lipids, Inc. (Alabaster, AL). Purity >99.5% was determined by thin-layer chromatography for phospholipids in chloroform/methanol/water=65:25:4 (by volume) and hexane/diethyl ether/chloroform=7:3:3 for cholesterol. All materials were used without further purification.

Measured stock solutions of the lipids and 16-PC in chloroform were mixed in a glass tube. The concentration of spin label was 0.2 mol% of the lipids. Multibilayer samples were prepared by the method of Rapid Solvent Exchange [16] in a buffer of PIPES/KCl/EDTA=5 mM:200 mM:1 mM at pH 7.0. Samples were then pelleted using a desktop centrifuge, and transferred to 1.5-mm I.D. capillaries with excess buffer. Samples were deoxygenated in a glove bag by

alternately pumping and adding N₂ gas over 3 h. Each capillary was flame-sealed.

2.2. ESR spectra measurement and simulation methods

ESR spectra were obtained on a Bruker Instruments EMX ESR spectrometer at a frequency of 9.55 GHz at room temperature (~24 °C).

Nonlinear least-squares (NLLS) fitting based on the stochastic Liouville equation [17,18] was performed for analyzing the spectra from 16-PC. The most relevant dynamic parameters used in the fitting program are the rotational diffusion rates (R_{\perp}) and the order parameter (S_0). Molecular axis systems and definitions have been well defined for spectral simulations of membranes [19]. The MOMD model, which stands for microscopic order and macroscopic disorder [20], was used in the simulations.

2.3. Tie-line determination

The tie-line determination method using spin-label ESR is based on linear combinations of experimental ESR spectra, which was originally used to determinate the partition coefficient (K_p) of 16-PC spin label in the two-component liquid-disordered (L_{α}) and gel (L_{β}) coexistence phase [15]. K_p was found to be invariant along the tie-line, as required by thermodynamics, by both spectral simulation and investigations using linear combinations of experimental data (see below for details). Here, we extend this approach to find the tie-lines in a two-phase coexistence region of a ternary mixture with the criterion that K_p is invariant along a tie-line.

In a two-phase coexistence region our tie-line method consists of two steps: First, a trial pair of boundary samples is selected. This trial pair defines a trial tie-line. Second, samples are prepared that fall on this proposed tie-line. The k^{th} experimental spectrum of these samples along the hypothetical tie-line is expressed in terms of a vector, $\mathbf{C}_{i,k}$. For analyzing spectra collected from samples on the trial tie-lines, each i^{th} spectrum vector is fit with a vector $\Phi_{i,k}$, which is composed of a pair of boundary spectral vectors, \mathbf{A}_i and \mathbf{B}_i , with component fraction $\gamma_{i,k}$ for \mathbf{A}_i and $(1-\gamma_{i,k})$ for \mathbf{B}_i (cf. Eq. (1)). The partition coefficient $(K_p)_{i,k}$ for the k^{th} spectrum on the i^{th} hypothetical tie-line is given in Eq. (2) below in terms of the lever rule prediction for the fraction $\mu_{i,k}$ of component \mathbf{A}_i and the estimated component fraction $\gamma_{i,k}$. A partition coefficient $(K_p)_{i,k}$ would be unity if the spin label partitions into each coexisting phase with equal concentration. A $(K_p)_{i,k}$ that is greater than unity would indicate the spin label favors the phase associated with spectral component \mathbf{A} . Eq. (3), derived from Eqs. (1) and (2) (by solving Eq. (2) for $\gamma_{i,k}$ in terms of $(K_p)_{i,k}$ and then substituting into Eq. (1)), shows the spectrum vector $\Phi_{i,k}$ expressed in terms of $(K_p)_{i,k}$, which must be constant for a true tie-line (i.e., $(K_p)_{i,k}$ is independent of k). The analysis would then be to find the single $(K_p)_i$ that is independent of

k and best matches the $\Phi_{i,k}((K_p)_i)$ with the $C_{i,k}$ for the set of all the spectra on the i^{th} hypothetical tie-line; (let us call the dimension of that set S_i). This would involve minimizing the $(\chi^2_{\text{red}})_{i,k}$ as defined in Eq. (4) for the set of S_i spectra, i.e., minimizing $\langle \chi^2_{\text{red}} \rangle_i$ defined in Eq. (4'), subject to the constraint of a single $(K_p)_i$ for all k . Note that N and P in Eq. (4) represent the number of points per spectrum and the number of fitting parameters, respectively. Some a priori knowledge of the experimental error is taken into consideration. The constant $(\sigma_N)_i$ in Eq. (4) represents the standard deviation of noise, for the i^{th} trial tie-line, estimated from the first and last 100 experimental points, corresponding to baseline, of the measured spectra in a set, i.e., spectrum vectors A_i , B_i and $\{C_{i,k}\}_{k=1, 2, \dots, S_i}$. A perfect match between experimental ($C_{i,k}$) and linearly combined spectra ($\Phi_{i,k}$) would be achieved as the $(\chi^2_{\text{red}})_{i,k}$ approaches unity. The procedure would need to be repeated for each trial tie-line, and then the best approximation to the true tie-line would be the one exhibiting the smallest $\langle \chi^2_{\text{red}} \rangle_i$.

$$\Phi_{i,k} = \gamma_{i,k} A_i + (1 - \gamma_{i,k}) B_i \quad (1)$$

$$(K_p)_{i,k} = \frac{\mu_{i,k}}{(1 - \mu_{i,k})} \times \frac{(1 - \gamma_{i,k})}{\gamma_{i,k}} \quad (2)$$

$$\Phi_{i,k}((K_p)_{i,k}) = \frac{\mu_{i,k}}{\mu_{i,k} + (K_p)_{i,k}(1 - \mu_{i,k})} A_i + \left[\frac{(K_p)_{i,k}(1 - \mu_{i,k})}{\mu_{i,k} + (K_p)_{i,k}(1 - \mu_{i,k})} \right] B_i \quad (3)$$

$$(\chi^2_{\text{red}})_{i,k} = \frac{1}{(N - P)(\sigma_N)_i^2} \left(C_{i,k} - \Phi_{i,k}((K_p)_i) \right)^T \times \left(C_{i,k} - \Phi_{i,k}((K_p)_i) \right) \quad (4)$$

$$\langle \chi^2_{\text{red}} \rangle_i = \frac{1}{S_i} \sum_{k=1}^{S_i} (\chi^2_{\text{red}})_{i,k} \quad (4')$$

However, we have found that this procedure is not very robust in providing a clearly defined minimum in $\langle \chi^2_{\text{red}} \rangle_i$. In our initial studies of the partition coefficient for the unique tie-line for DPPC/DLPC binary mixtures (see below), we found that such a procedure suffers from experimental inaccuracy, e.g., prepared lipid concentrations not exactly on the hypothetical tie-line and noise in spectral collections. Thus, we found it best not to fix $(K_p)_{i,k}$ in fitting the spectra along the i^{th} presumed tie-line. Instead, each spectrum ($C_{i,k}$) along the i^{th} hypothetical tie-line was fit to its own optimum $(K_p)_{i,k}$ and linear combination of boundary spectra. Then the $\langle \chi^2_{\text{red}} \rangle_i$ for this presumed tie-line was calculated according to Eq. (4'). To correct this $\langle \chi^2_{\text{red}} \rangle_i$ for the fact that $(K_p)_{i,k}$ must be independent of k along a true tie-line, we determined $\langle K_p \rangle_i$ (i.e., the average $(K_p)_{i,k}$ over the S_i spectra along the i^{th} hypothetical tie-line) and its standard deviation, $\langle \sigma_{Kp} \rangle_i$,

and then we multiplied the $\langle \chi^2_{\text{red}} \rangle_i$ with a normalized $(\sigma_{Kp})_i$ (given as the second term on the right-hand side of Eq. (5)) for the i^{th} hypothetical tie-line where M represents the number of hypothetical tie-lines in a set:

$$(\chi^2)_i \equiv \langle \chi^2_{\text{red}} \rangle_i \times \frac{(\sigma_{Kp})_i}{\min \{ (\sigma_{Kp})_{i=1,2,\dots,M} \}} \quad (5)$$

We found that this $(\chi^2)_i$ given by Eq. (5) (which is determined by both $\langle \chi^2_{\text{red}} \rangle_i$, which measures the spectral fitting in the two-phase region, and $(\sigma_{Kp})_i$, which measures how much $(K_p)_{i,k}$ varied in achieving this fit) is a robust indicator, whose minimum can be taken to distinguish the best approximation to the true tie-line, as we discuss below.

3. Results

The ternary phase diagram of DPPC/DLPC/Chol at 24 °C shown in Fig. 1 was determined by Feigenson and Buboltz [14]. Only those names of the phases that are of importance to the present study are noted. The boundaries of the two-phase coexistence region of $L_\alpha + L_\beta$ have been well established by use of FRET and confocal fluorescence microscopy [14]. ESR has revealed the dynamic molecular structure of much of the phase diagram [15]. However, the direction of the tie-lines in the two-phase coexistence region of the L_α and L_β phases (cf. Fig. 1) was not previously determined by any method. To determine the direction of tie-lines in this region, we made 21 hypothetical tie-lines at various angles to the DPPC/DLPC axis, examining over 100 samples. First, we tested the proposed method by examining the tie-line for the DPPC/DLPC binary mixtures. It is known

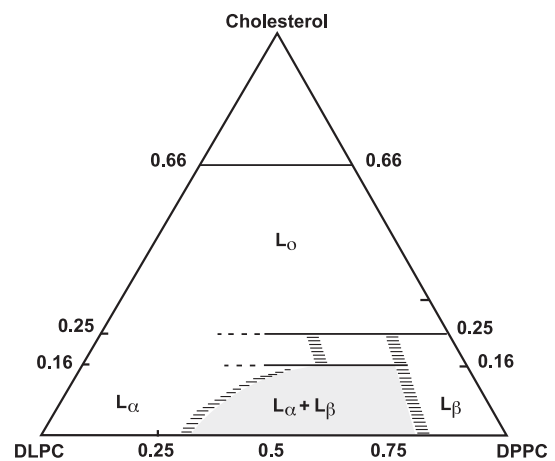


Fig. 1. Ternary phase diagram for DPPC/DLPC/Chol, at 24 °C. Each vertex represents a pure component in excess buffer. The numbers labeling the DLPC–DPPC axis correspond to $X_{\text{DPPC}}^{\text{PC}}$ whereas the numbers labeling the PC–cholesterol axes correspond to $X_{\text{chol}}^{\text{PC}}$ and indicate the values associated with various horizontal phase boundaries. This phase diagram is directly cited from Feigenson and Buboltz [14]. Names of the phases, which are of importance to the present study, are noted on the diagram. The shaded region is where the tie-lines are investigated in the present study.

in advance as the horizontal 0% cholesterol ($X_{\text{Chol}}=0$) line in the phase diagram of Fig. 1, but we compare it to other presumed tie-lines. Then we used this method to determine tie-lines for ternary mixtures including cholesterol. The objectives are: (1) to determine the directions of the tie-lines in the L_α and L_β coexistence region for different amounts of cholesterol; and (2) to determine the partition coefficient of 16-PC spin label in this coexistence region for each tie-line.

3.1. Demonstration of the tie-line determination method

A test of the method was performed by preparing samples that fall on five trial tie-lines in the vicinity of the true tie-line at $X_{\text{Chol}}=0$. The five trial lines are X_{Chol} =(from fluidus L_α to solidus L_β boundary) 0–0%, 0–1%, 0–2%, 1–0%, and 2–0%.

The results are shown in Table 1. The first column of Table 1 gives the cholesterol concentration (X_{Chol}) on the fluidus boundary, while the second column gives X_{Chol} on the solidus boundary. They represent a pair of boundary samples, i.e., the trial conjugate phases, locating the ends of each hypothetical tie-line. $\langle K_p \rangle$, given in the third column, is the average of the best-fit partition coefficients for the samples on each hypothetical tie-line, with σ_{K_p} its standard deviation. The criterion used to determine the best choice of tie-line is the minimum in the (χ^2) value given in the last column. The known tie-line, 0–0%, is correctly determined by this procedure and is highlighted in boldface in Table 1. The K_p for 16-PC along the correct tie-line is approximately unity (1.1 ± 0.1). Thus, the method based on the χ^2 criterion yields the correct tie-line and clearly distinguishes it from other choices of tie-line, which differ only slightly in boundary composition.

3.2. Determination of tie-lines in the L_α and L_β coexistence region

The 16 hypothetical tie-lines that we studied are summarized in Table 2. The 16 hypothetical lines are

Table 1

A test of the method on the samples that fall on five trial tie-lines in the vicinity of the true tie-line

X_{Chol,L_α} (%) ^a	X_{Chol,L_β} (%) ^b	$\langle K_p \rangle$ ^c	σ_{K_p} ^d	$\langle \chi^2_{\text{red}} \rangle$ ^e	$(\chi^2)_i$ ^f
0	1	0.79	0.11	35.2	38.7
0	2	0.98	0.16	46.2	73.9
0	0	1.14	0.10	21.2	21.2
1	0	1.09	0.16	20.7	33.1
2	0	1.12	0.21	17.6	36.9

^a Cholesterol mole concentration of the sample on the fluidus L_α boundary.

^b Cholesterol mole concentration of the sample on the solidus L_β boundary.

^c Average partition coefficient, K_p , over the S_i spectra along the i^{th} trial tie-line.

^d Standard deviation of the partition coefficients.

^e Average reduced Chi-squared values, defined in Eq. (4').

^f Defined in Eq. (5), representing χ^2 value in the i^{th} trial tie-line.

Table 2

The tie-lines determined in the region of two-phase coexistence in a ternary lipid mixture

X_{Chol,L_α} (%) ^a	X_{Chol,L_β} (%) ^b	$\langle K_p \rangle$ ^c	σ_{K_p} ^d	$\langle \chi^2_{\text{red}} \rangle$ ^e	$(\chi^2)_i$ ^f
4	7	1.06	0.41	49	670
	6	1.05	0.14	48	224
	5	1.15	0.10	65	217
	4	0.95	0.03	90	90
8	11	5.67	8.07	26	499
	10	1.87	0.72	56	96
	9	1.34	0.42	34	34
	8	2.09	2.34	23	128
12	15	1.69	0.52	84	84
	14	2.25	1.34	34	87
	13	1.86	0.66	15	19
	12	1.91	1.18	16	36
13	16	1.38	0.48	21	21
	15	1.79	0.49	9.6	9.8
	14	1.61	0.51	16	17
	13	1.94	1.01	21	44

a,b,c,d,e and f are noted in Table 1.

organized into four sets in order to determine four tie-lines running from the fluidus boundary with cholesterol concentrations at $X_{\text{Chol}}=4\%$, 8% , 12% and 13% to the solidus boundary in the two-phase coexistence region. The χ^2 criterion clearly distinguishes a best choice for the correct tie-line from other similar compositions. These best choices are in boldface in Table 2.

Fig. 2 shows the five tie-lines (including the 0–0% tie-line) that we determined by this method. For simplicity of presentation, only those samples on the “best-choice” tie-lines and on the boundaries are shown, although over 100

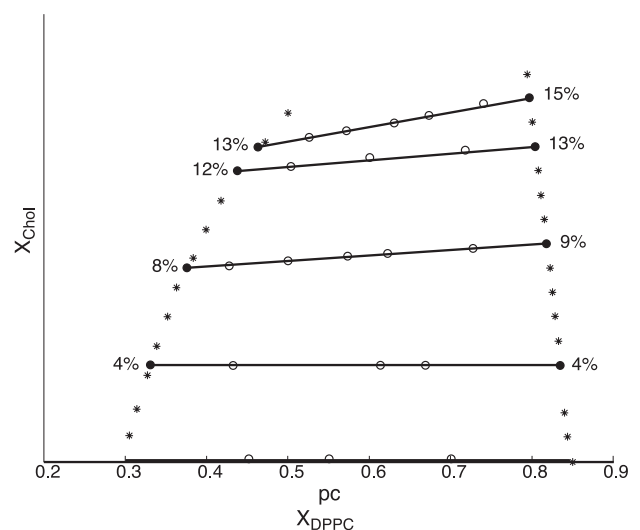


Fig. 2. Enlarged plot of the two-phase coexistence region in Fig. 1. The five determined tie-lines obtained using the tie-line determination method are shown by solid lines. They are X_{Chol} (cholesterol mole concentration from fluidus to solidus boundaries)=0–0%, 4–4%, 8–9%, and 13–15%, as noted on the figure. Samples within the two-phase coexistence region of the L_α and L_β are shown by circles. Samples along the phase boundaries are shown by asterisks. The slope of the tie-line relative to the $X_{\text{DPPC}}^{\text{PC}}$ axis is found to slightly increase with cholesterol concentration varying from 0% to 15%.

samples in total were examined. Sample points shown in Fig. 2 are plotted in the triangular coordinates, best illustrated in Fig. 1, to precisely locate the positions of the sample compositions. The $(\chi^2)_i$ values in Table 2 show how well the samples along these tie-lines in the two-phase region are fit with a pair of boundary spectra, and the requirement of constant K_p .

In the region of low cholesterol concentration, at $X_{\text{Chol}}=4\%$, we find that the tie-line is parallel to the phase diagram boundary of the binary DPPC/DLPC mixtures, i.e., $X_{\text{Chol}}=0$. Furthermore, this analysis shows that with just a 1% cholesterol increase on the solidus boundary (i.e., the line going from $X_{\text{Chol}}=4\%$ on the fluidus boundary to $X_{\text{Chol}}=5\%$ on the solidus boundary), χ^2 increases by a factor of 2.4 as compared to the tie-line running from $X_{\text{Chol}}=4\%$ to 4%. This is a remarkable sensitivity to the tie-line direction. For cholesterol concentrations 8% or higher, the tie-lines are tilted slightly with a positive slope relative to the DPPC/DLPC axis. The higher the cholesterol concentration, the more positive the slope. The other tie-lines are found to run (from fluidus to solidus) $X_{\text{Chol}}=8\text{--}9\%$, $12\text{--}13\%$, and $13\text{--}15\%$.

3.3. Partition coefficient variation with varying cholesterol concentration

In addition to the slightly changing slope of the tie-lines determined from our analysis, K_p of 16-PC was found to differ for the different tie-lines. K_p of 16-PC for the tie-lines $X_{\text{Chol}}=0\text{--}0\%$ and $4\text{--}4\%$ are 1.1 ± 0.1 and 0.95 ± 0.03 , respectively, and are in good agreement with the K_p for the $0\text{--}0\%$ tie-line found in our previous study (0.88 ± 0.24 ; Ref. [15]). This result shows approximately equal partitioning of 16-PC in the L_α and L_β two-phase coexistence region in binary mixtures of DPPC and DLPC. In the present study, K_p for the tie-lines $X_{\text{Chol}}=8\text{--}9\%$, $12\text{--}13\%$, and $13\text{--}15\%$ were found to be 1.3 ± 0.4 , 1.9 ± 0.7 , and 1.8 ± 0.5 , respectively. An interesting observation is that K_p does not approach unity as one might expect if the two phases are approaching a plait point with increasing X_{Chol} . This observation leads to the questions: (1) Does a K_p different from unity imply that the two conjugate phases in the high cholesterol region are dissimilar as is true in the low cholesterol region? (2) What are the implications of the absence of a plait point near the boundary of $\sim 16\%$? We consider these two questions in the discussion section.

3.4. The dynamic molecular structure of the phase boundaries

The dynamic structures for the fluidus and solidus boundaries are shown in Fig. 3 in terms of rotational diffusion rates R_\perp and order parameter S_0 . These dynamic parameters obtained from fitting the samples at the ends of the determined tie-lines (i.e., along the boundaries) are shown by solid lines marked with squares and circles,

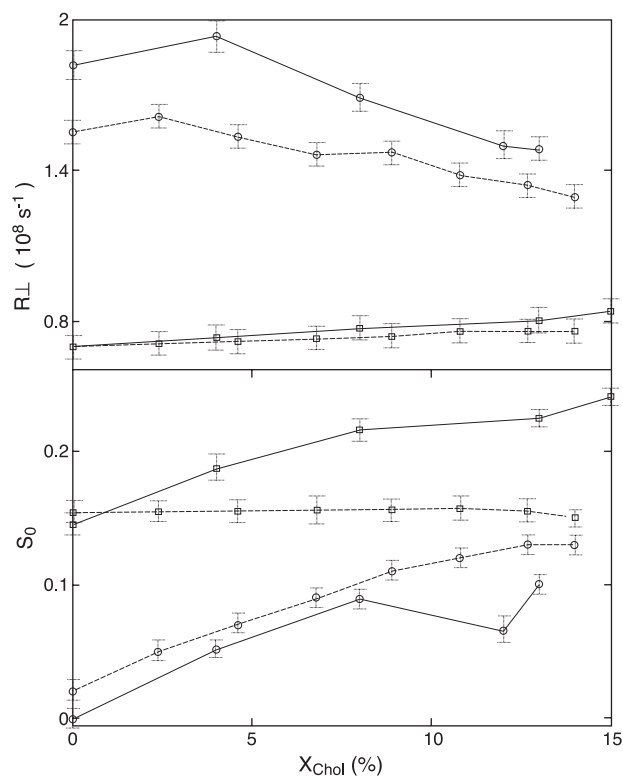


Fig. 3. The dynamic molecular structures of the phase boundaries, expressed in terms of the dynamic parameters R_\perp and S_0 . The dynamic parameters obtained from spectral fitting are shown by solid lines with squares and circles, representing solidus and fluidus boundaries, respectively. For comparison, the theoretical predictions obtained in the previous study [15] are also shown by dashed lines with same definitions for squares and circles. The estimated errors for R_\perp and S_0 are ca. 5% and 1%, respectively.

respectively representing the samples on the solidus and fluidus boundaries. The R_\perp on the fluidus boundary decreases slightly from $1.82 \times 10^8 \text{ s}^{-1}$ at $X_{\text{Chol}}=0\%$ to $1.48 \times 10^8 \text{ s}^{-1}$ at $X_{\text{Chol}}=13\%$, while on the solidus boundary it remains at about $0.75 \times 10^8 \text{ s}^{-1}$ within the same range of cholesterol concentration. The order parameter S_0 increases by about 0.1 along the solidus and fluidus boundaries with increased cholesterol. That is, S_0 on the fluidus boundary increases from 0 at $X_{\text{Chol}}=0\%$ to 0.1 at $X_{\text{Chol}}=13\%$, whereas S_0 on the solidus boundary increases from 0.145 to 0.24 within the same range. Thus, adding cholesterol into either the L_α or L_β phase results in a similar magnitude of change in molecular ordering (S_0) along the boundaries. It must be noted that although there is the same magnitude of change in ordering, the angular change ($\delta\theta$) in the L_α phase is actually larger than that in the L_β phase (4.2° vs. 3.6°).

For comparison, the dynamic parameters of the boundaries obtained from the theoretical prediction in our previous study are shown by dashed lines in Fig. 3 [15]. Note that the “theoretical prediction” here means that the two spectral components that represent a pair of conjugate phases at the end points of an assumed tie-line were obtained from fitting an experimental spectrum within the

two-phase region to two spectral components, and then assigning these components on the assumption that the tie-lines in this two-phase region are parallel to the $X_{\text{Chol}}=0\%$ tie-line. As shown in Fig. 3, the dynamic parameters of the boundaries obtained from the theoretical predictions are still in reasonable agreement within experimental uncertainty with the present study obtained from actually fitting the spectra along the boundaries. The only exception is that the order parameter S_0 on the solidus boundary varies more than the previous predictions. This difference undoubtedly results from the tie-line direction not having previously been carefully investigated, and K_p for 16-PC having been assumed to be constant. The present study implies that accurately determining the tie-lines and the variation of K_p for different tie-lines is essential for accurately determining the dynamic parameters of the true conjugate phases.

4. Discussion

4.1. Characteristics of the tie-line determination method

We have developed a generally applicable method to find thermodynamic tie-lines. This method is based on the facts that the spectra on a tie-line can be formed as a linear combination of the two boundary spectra, constrained by the lever rule, and K_p is invariant along a tie-line.

The dissimilarity of the boundary spectra is a major characteristic that makes the tie-line determination useful using linear combinations of ESR experimental spectra. ESR of spin-labeled lipids is characterized by significant line shape changes, because the motion of the probe molecule is in the regime of slow motion. In Fig. 4, two pairs of boundary spectra for the tie-lines, (a) $X_{\text{Chol}}=13\text{--}15\%$ and (b) $X_{\text{Chol}}=0\text{--}0\%$, are plotted to illustrate how different are the line shapes of the boundary spectra. The boundary spectra for the tie-line in either the low or high cholesterol region are very dissimilar. Because any spectrum along a tie-line in the two-phase region is a superposition of the pair of boundary spectra at the ends of the tie-line, the more dissimilar a pair of boundary spectra the more likely the component fractions ($\gamma_{i,k}$ in Eq. (1)) are accurately obtained. In other words, selecting a particular spin label that displays large differences in the local environments of the respective conjugate phases is essential in order to employ the proposed method. The differences in the boundary spectra indicate that the spin label 16-PC displays sufficient differences in the local environments of the two coexisting phases with variation in cholesterol concentration.

In addition, the method relies on there being a variation of the ESR spectrum along the phase boundaries, which is observable although necessarily small for adjacent ESR spectra corresponding to a 1% change in X_{Chol} but there are small fluctuations as expected from small imprecisions in

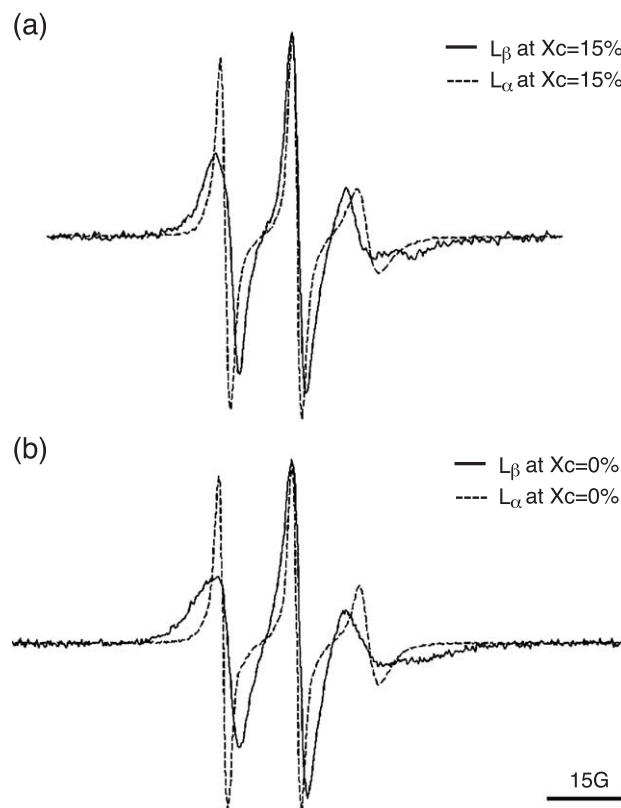


Fig. 4. The experimental boundary spectra that locate the end points of the tie-lines $X_{\text{chol}}=(a)$ 13–15% and (b) 0–0%. The end-chain labeled phospholipid 16-PC exhibits substantially different ESR spectra for the two respective conjugate phases.

sample composition and spectral collections. These small experimental variations are probably the reason (in addition to those noted above) that Eq. (4') is not, in itself, a very precise criterion for determining the tie-lines, but, as we have seen, it is successful in conjunction with minimizing the variance in K_p .

4.2. Implications of the partition coefficients

The partition coefficients for the tie-lines $X_{\text{Chol}}=12\text{--}13\%$ and $13\text{--}15\%$ are found to be 1.9 ± 0.7 and 1.8 ± 0.5 , showing no evidence of approaching unity as the boundary at $X_{\text{Chol}} \sim 16\%$ is reached. The boundary spectra at the end points of the 0–0% and 13–15% tie-lines illustrated in Fig. 4 are clearly dissimilar, as are the associated dynamic parameters, R_{\perp} and S_0 , shown in Fig. 3. A key question raised by these results is why the conjugate phases do not become more similar as one approaches the boundary where a plait point is expected [14]. Most likely, there is no plait point on the boundary $X_{\text{Chol}} \sim 16\%$. Instead, we suspect this boundary is a separation between a two-phase region of $L_{\alpha}+L_{\beta}$ phases and a three-phase region of $L_{\alpha}+L_{\beta}+L_o$ phases, which exists above the $X_{\text{Chol}} \sim 16\%$ boundary. Any such three-phase coexistence regions must be a triangle—surrounded by three straight lines, all of which are necessarily tie-lines of the three two-phase coexistence

regions, inferred from the contact rule for phase regions [21–23].

5. Summary

A novel method for determining the tie-lines in coexisting membrane phases of a ternary lipid vesicle system has been presented. Over 100 samples within the $L_{\alpha}+L_{\beta}$ two-phase coexistence region exhibited by DPPC/DLPC/Chol and along the boundaries were investigated to apply this method. By studying this two-phase coexistence region, we determined the tie-lines and determined the dynamic molecular structures of the boundaries using linear combinations of ESR experimental data and spectral fitting. The success of the method depends on having a spin label which (1) exhibits significantly different ESR spectra in the two phases, and (2) partitions well into both coexisting phases.

In addition, the partition coefficient of the spin-label (16-PC) was determined for each tie-line. In the low cholesterol concentration region $\leq 4\%$, K_p was found to be approximately unity. Interestingly, the 16-PC K_p at high cholesterol concentrations was found to be ~ 1.5 – 2 . This observation, along with the dissimilarity of the ESR spectra from the two conjugate phases, implies that no plait point is approached, and that instead the $L_{\alpha}+L_{\beta}$ phase coexistence is interrupted by the appearance of a new phase. Hence, as a result of quantitative K_p and tie-line determination, a region of three-phase coexistence is strongly implied.

Spin-label ESR is thus found to be unique in the field of lipid membranes in its utility for determining tie-lines in coexisting membrane phases and in extracting dynamic structural parameters associated with these phases.

References

- [1] K. Simons, E. Ikonen, Functional rafts in cell membranes, *Nature* 387 (1997) 569–572.
- [2] S.L. Veatch, S.L. Keller, Separation of liquid phases in giant vesicles of ternary mixtures of phospholipids and cholesterol, *Biophys. J.* 85 (2003) 3074–3083.
- [3] T. Baumgart, S.T. Hess, W.W. Webb, Imaging coexisting fluid domains in biomembrane models coupling curvature and line tension, *Nature* 425 (2003) 821–824.
- [4] C. Dietrich, L.A. Bagatolli, Z.N. Volovyk, N.L. Thompson, M. Levi, K. Jacobson, E. Gratton, Lipid rafts reconstituted in model membranes, *Biophys. J.* 80 (2001) 1417–1428.
- [5] M. Ge, A. Gidwani, H.A. Brown, D. Holowka, B. Baird, J.H. Freed, Ordered and disordered phases coexist in plasma membrane vesicles of RBL-2H3 mast cells. An ESR study, *Biophys. J.* 85 (2003) 1278–1288.
- [6] S.L. Veatch, I.V. Polozov, K. Gawrisch, S.L. Keller, Liquid domains in vesicles investigated by NMR and fluorescence microscopy, *Biophys. J.* 86 (2004) 2910–2922.
- [7] L. Alder, *Liquid–Liquid Extraction*, 2nd ed., Elsevier, Amsterdam, 1959.
- [8] W. Bancroft, S.S. Hubbard, A new method for determining diner distribution, *J. Am. Chem. Soc.* 64 (1942) 347.
- [9] D.F. Othmer, P.E. Tobias, Toluene and acetaldehyde systems; tie line correlation; partial pressures of ternary liquid systems and the prediction of tie lines, *Ind. Eng. Chem.* 34 (1942) 690–700.
- [10] A.W. Francis, *Liquid–Liquid Equilibriums*, Interscience Pub., New York, 1963.
- [11] T. Magnussen, J.M. Sorensen, P. Rasmussen, A. Fredenslund, Liquid–liquid equilibrium data—their retrieval, correlation and prediction. 3. Prediction, *Fluid Phase Equilib.* 4 (1980) 151–163.
- [12] J.M. Sorensen, T. Magnussen, P. Rasmussen, A. Fredenslund, Liquid–liquid equilibrium data—their retrieval, correlation and prediction. 1. Retrieval, *Fluid Phase Equilib.* 2 (1979) 297–309.
- [13] J.M. Sorensen, T. Magnussen, P. Rasmussen, A. Fredenslund, Liquid–liquid equilibrium data—their retrieval, correlation and prediction. 2. Correlation, *Fluid Phase Equilib.* 3 (1979) 47–82.
- [14] G.W. Feigenson, J.T. Buboltz, Ternary phase diagram of dipalmitoyl-PC/dilauroyl-PC/cholesterol: Nanoscopic domain formation driven by cholesterol, *Biophys. J.* 80 (2001) 2775–2788.
- [15] Y.W. Chiang, Y. Shimoyama, G.W. Feigenson, J.H. Freed, Dynamic molecular structure of DPPC–DLPC–cholesterol ternary lipid system by spin-label electron spin resonance, *Biophys. J.* 87 (2004) 2483–2496.
- [16] J.T. Buboltz, G.W. Feigenson, A novel strategy for the preparation of liposomes: rapid solvent exchange, *Biochim. Biophys. Acta, Biomembr.* 1417 (1999) 232–245.
- [17] D.E. Budil, S. Lee, S. Saxena, J.H. Freed, Nonlinear-least-squares analysis of slow-motion EPR spectra in one and two dimensions using a modified Levenberg–Marquardt algorithm, *J. Magn. Reson., Ser. A* 120 (1996) 155–189.
- [18] D.J. Schneider, J.H. Freed, in: L.J. Berliner, J. Reuben (Eds.), *Spin Labeling: Theory and Application*, Plenum, New York, 1989, pp. 1–76.
- [19] M.T. Ge, J.H. Freed, Electron-spin resonance study of aggregation of gramicidin in dipalmitoylphosphatidylcholine bilayers and hydrophobic mismatch, *Biophys. J.* 76 (1999) 264–280.
- [20] E. Meirovitch, A. Nayeem, J.H. Freed, Analysis of protein lipid interactions based on model simulations of electron-spin resonance spectra, *J. Phys. Chem.* 88 (1984) 3454–3465.
- [21] L.S. Palatnik, A.I. Landau, *Phase Equilibria in Multicomponent Systems*, Holt, Rinehart and Winston, Inc., 1964.
- [22] L.S. Palatnik, A.I. Landau, *Issledovanie Protseessov, Protekayushchikh S Izmeneniem Chisla Stepenei Svobody V Mnogokomponentnykh Geterogennykh Sistemakh*. 1, *Zh. Fiz. Khim.* 29 (1955) 1784–1803.
- [23] L.S. Palatnik, A.I. Landau, *Topologicheskoe Issledovanie Diagramm Ravnovesiya Mnogokomponentnykh Geterogennykh Sistem I Ikh Neuzlovykh Sechenii Pri Pomoshchi Pravila O Soprikasayushchikh-sya Oblastyakh Razdeleniya*. 1, *Zh. Fiz. Khim.* 30 (1956) 2399–2411.